CHAPTER 1

Propulsion Elements for Solid Rocket Motors

ROLAND LUCAS

1. Principles of Propulsion

1.1. INTRODUCTION

Rocket launches have become a familiar spectacle. Newspapers, movies and television frequently show us the images of the first moments of lift-off. Impressed by the large quantity of gases released at the lift-off of the rocket, a knowledgeable spectator will deduce the relationship between cause and effect. As a perceptive observer he will have in fact discovered the principle of propulsion, which links reaction force to the ejection of a mass.

Expressed by an equation and applied to rockets, this principle is:

$$F = q \cdot Ve$$

where F is the reaction force which we call thrust, q is the gas mass flow rate and Ve the exhaust velocity of the gases.

Following his logical line of reasoning, the observer will then wonder about the origin of such a volume of gas ensuring for many seconds the propulsion of the rocket. If his creative mind leads him to think of the burning of a solid mass, on board the rocket, he will then have imagined the concept of solid fuel rockets.

1.2. MAIN COMPONENTS OF A ROCKET MOTOR

The rocket motor (Fig. 1) is designed to ensure the combustion under pressure of the propellant grain it contains. The resulting gases are expanded through the nozzle, whose function is to convert this pressure into supersonic exhaust.

As a rule, such a rocket motor has five major components.

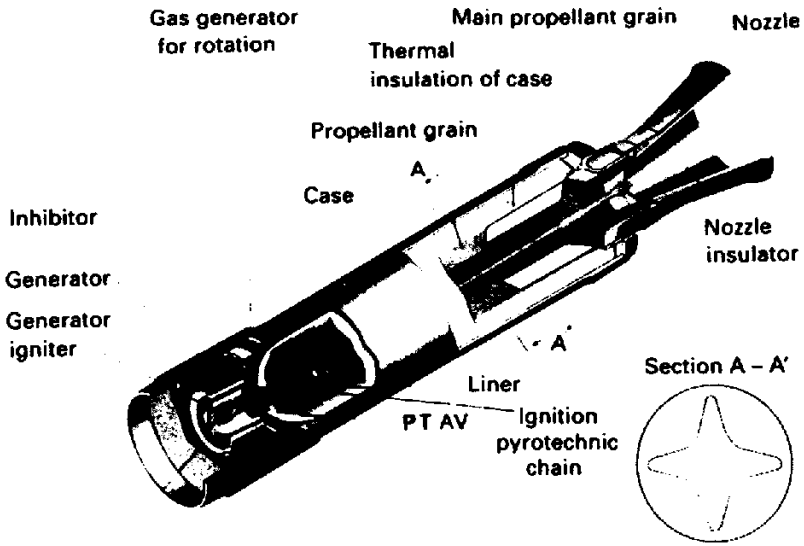

FIG. 1.1. Typical rocket motor.

1.2.1. *The case*

Made either from metal (high-resistance steels) or from composite materials by filament winding (glass, kevlar, carbon), the case must be capable of withstanding the internal pressure resulting from the motor operation, approximately 3–25 MPa, with a sufficient safety coefficient, usually of the order of 1.4.

1.2.1.1. Ballistic missiles and space launchers

For ballistic missiles and space launchers, special industrial resources have been developed to manufacture cases with an internal volume of up to about 10 cubic meters.

(a) Metal cases

Several types of steel are used for the metal cases (such as AMS 6487 or AMS 6520) whose main characteristics are their great mechanical strength, usually greater than 1000 MPa, and the ease with which they can be shaped.

For the cylindrical body, two manufacturing methods are used:

- wrapping-welding of long steel sheets, requiring longitudinal welding;
- flow turning of rough forgings, avoiding the drawback of welding and offering the possibility of progressive thicknesses.

The technique used for the production of the end closures of the cases involves the machining of solid thermal press forgings. Consequently grooves for handling, and for the interfacing between the various stages, can be obtained from a solid steel block. The end closures and cylindrical body are welded together. The additional manufacturing cycles involve various thermal treatments (hardening, tempering), finish machining, surface treatments (anti-corrosion) and a pressurization test above the maximum expected operating pressure (over-test coefficient of the order of 1.15).

Quality control testing is performed at every stage of the manufacture, including tests of metal properties, X-ray and ultrasonic testing [1].

(b) Composite material cases

The so-called filament-wound cases use composite materials spun into filaments (glass, kevlar, carbon) and a matrix consisting of thermosetting resin of a polyester, epoxide or polyamide type. An overview of these composite materials for propulsion application is shown in ref. [2].

Based on the internal pressure requirements during operation, the design analysis of a case of this type is done in two stages: a preliminary design phase, followed by a testing phase [3]. The first phase is based on the principle that the case has rigidity only in the direction of the filaments. Geometry, corresponding thicknesses, as well as the winding law ensuring the fiber stability requirement (elimination of the risk of slippage during the winding) can be rapidly determined. The second stage uses the computational methods with finite elements by considering the material as a homogeneous orthotropic solid, and enables verification of the structural integrity of the whole.

Once the design has been completed, and the manufacturing parameters determined, manufacture of the case may begin. The fibers, impregnated with resin, are wound on a mandrel shaped as required with the help of a special lathe. The mandrel, an agglomerate of sand, or a metallic piece fitting, is first coated with the thermal insulation intended for the case and is equipped with metal polar bosses at both ends. These metal bosses help strengthen the forward and aft openings and provide the connection with the other components, such as the ignition system and the nozzle. There are two winding methods: the wet process which involves continuous impregnation during manufacture or the dry process, which uses previously impregnated fibers. Two successive types of filament winding are necessary:

- the first filament winding is a succession of loops tangential to the two openings: this is "helix" or "polar" winding, designed to cover the domes and the case;
- the second filament winding covers only the cylindrical section, perpendicular to the generatrix: this is the "hoop" winding.

The entire part is then cured in an oven, with temperature (from 60° to 150°C) and duration (approximately 20 h) depending on the material used; then the mandrel is removed. If it is an agglomerate of sand, a hydraulic process is used to disintegrate the mandrel. The manufacturing process ends with final machining. A series of tests is performed before delivery, i.e., ultrasound tests for structural integrity of the winding and the bonding of the internal thermal insulation.

1.2.1.2. Tactical missiles and rockets

Similar manufacturing processes are used for both tactical missiles and rockets. A comparison between metal cases and cases made of fiber-reinforced plastics is provided in ref. [4].

(a) Metal cases

The selection of manufacturing technique is based on the performance requirements and includes:

- Helical wrapped-welded techniques, which are very well suited for large industrial production.
- Wrapped-welded techniques along the length of the generatrix, used for mid-size or small production runs;
- Flow forming, which does away with the drawbacks of welding along the generatrix and has the advantage of very good precision and very good inside surface conditions — this technique can be used for large-scale production but requires substantial investments.
- Metallic strips which are first coated with an adhesive and then wound in an helical configuration on a mandrel [5]. The number of layers wound is a function of the thickness desired. This technique allows the manufacture of metal cases with a very high level of mechanical strength under normal operational conditions and, according to the inventors of the process, shows specific advantages in the field of insensitive munitions. In the case of unplanned stimuli (fire, bullet impact) resulting in the ignition of the propellant inside the case, the strip laminate technique prevents the usual explosion caused by confinement of the gases until rupture. Composite material cases may offer similar advantages.

As a rule the manufacturing processes described above require that the end closures, which are press-forged and machined, be welded to the case. Sometimes the assembly of the forward end closure and the case, press-forged, is accomplished by a flow forming process to minimize the number of weld beads.

Because of the scale of industrial production, manufacturing costs require the use of metal that can be welded and machined, and that is not too

expensive. Steel type AMS 6520 is commonly used for tactical engines. The machining technology for this type of steel allows a minimum thickness of approximately 1 mm.

Aluminum-copper (AMS 2014) and aluminum-zinc-magnesium (AMS 7075) alloys are also used for small-caliber rockets.

(b) Wound composite material cases

Specific performance characteristics of metals (modulus E and maximum strength σ_R divided by density ρ) are at best equal or inferior to the characteristics of wound fiberglass. Composite materials such as glass-epoxy, kevlar-epoxy and carbon-epoxy are used when performance requirements are important. However, with these materials, strain/stress induced through pressurization or TVC loads induced by ignition or TVC, may lead to significant hoop strains (1-2%), causing greater problems for the structural integrity of the propellant grain. Nevertheless, the winding technique is increasingly used for the production of tactical missile cases [6,7], and rockets [8]. The French company "Société Européenne de Propulsion" [9] has developed an interesting process using a method called structural assembly. The casting-curing cycle of the propellant grain is done in a rubber tube. The whole, serving as a mandrel, is then wrapped with impregnated filaments, thereby integrating the forward- and aft-end closures and, if necessary, a blast tube.

1.2.2. Propellant grain

Two main configurations — free-standing grain and case-bonded grain — with various central port geometries are used to fulfill the required performance objectives.

- Free-standing grains. Free-standing grains are contained inside a cylindrical plastic cartridge (PVC, etc.). They are secured inside the case by various support elements such as wedges, springs or grids.
- Case-bonded grains. These are obtained by casting the propellant, before polymerization has occurred, directly into a case already provided with thermal insulation. Additional manufacturing steps (molding, curing, machining, control) required for the propellant grain are performed on the loaded case.

1.2.3. Thermal insulation

The combustion temperature of propellant grains, ranging from approximately 1500 to 3500 K, requires the protection of the inside surface of the case.

The design of the internal insulation involves the following four major steps [10]:

- analysis of the internal thermal insulation environment: the nature of the propellant gases, internal aerodynamics, etc.;
- selection of the material: reduced scale tests designed to assess specimens in conditions simulating firing are performed;
- determination of the thickness in the various areas of the case necessary to withstand the heat;
- determination of the dimensions and thickness needed to withstand mechanical strains on the case and propellant grain.

In areas where flow erosion is high (high gas velocity in the vicinity of the case wall), dense and possibly even rigid materials made of asbestos, silicate and carbon fibers impregnated with a heat-proof resin (phenolic, polyamide) may be used. Today, however, elastomers are being increasingly preferred to these types of material. The use of elastomers has allowed significant improvements in insulation by the addition of a reinforcing filler. Due to the ban on asbestos filler, which has been used for many years, alternate insulation materials have been developed as a replacement for the asbestos-containing materials [11]. These reinforcing fillers are either in the form of fibers (silicate, kevlar and carbon) or in the form of powder fillers (silicate and carbon). Various densities can be obtained, in order to decrease the weight of inert parts in the motor.

Thermal insulation for the cylindrical part of the case, which is exposed only at the end of burning, can be provided by the liner, a rubber compound with low fillers that is sprayed. The liner's main function is to allow a good bond between the propellant and the case or the thermal rubber compound. Industrial production and the characteristics of this type of material are specifically discussed in Chapter 13.

1.2.4. *The nozzle*

The general shape of a nozzle (Fig. 2), called the nozzle profile, includes three major parts:

- the convergent zone of the nozzle, which channels the flow of propellant combustion gases;
- the throat: selection of throat dimensions determines the operating point of the rocket motor;
- the exit cone of the nozzle, which increases the exhaust velocity of the gases in their expansion phase, consequently improving the propulsive effect.

Since 1970, thermal and physical property improvements of the materials with, on the one hand, developments of new computer codes and, on the other hand, performance of experimental studies, have made possible important nozzle design improvements [12]. Currently, the shape and complexity of a nozzle depend on the expected level of performance and on the field of application of the rocket motor (space, ballistic missiles, tactical missiles). Its design requires knowledge of the following parameters [13]:

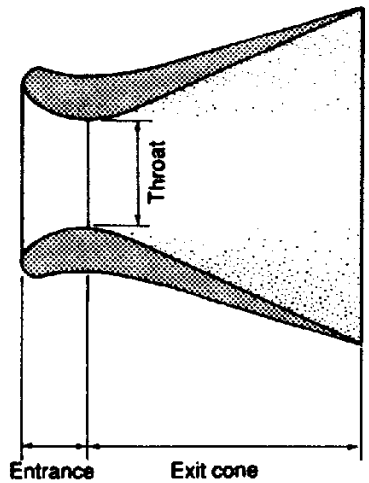

FIG. 1.2. Nozzle diagram.

- Internal operating pressure of the motor, which affects the structural integrity of the nozzle and the ablation of the thermal materials.
- Burning time, often negligible for small rocket motors (a few seconds) but in the case of large rocket motors (measured by the minute) an essential factor in the determination of the thickness required to withstand thermal transfer.
- Throat diameter, which will determine the operating pressure.
- Type of propellant used: the gases and the propellant's burning temperature determine the selection of the thermal materials.
- Space available; often a function of equipment necessary for the guidance of the missile; for example, the nozzles located at the end of a blast tube on some tactical engines.
- Expansion ratio (exit cone area A_s versus nozzle throat area A_t, i.e. $\varepsilon = A_s/A_t$) must allow a pressure in the exit section equal to the ambient pressure to allow maximum efficiency. Because space is usually limited on ballistic missiles, the concept of the extendible nozzle exit cone (during flight) permits an increase in this ratio during operation.
- Submergence of the nozzle into the burning chamber, defined as the ratio of the integrated length versus total length, to minimize the external part of the nozzle. This technology is used particularly on ballistic and space

missiles. The external nozzle, less complex technologically and less costly, is used for the propulsion of tactical missiles and in situations where overall vehicle length is not a constraint. The nozzle is sometimes placed at the end of an insulated metal tube. Use of this blast tube provides space for the devices that activate the steering controls of the missile.

- Thrust vector control which, in ballistics and space motors, uses the principle of a movable nozzle permitting thrust vector control angles ranging from 3° to 15°. The various mechanical systems used include flexible bearing, ball and socket, hydraulic bearing and rotatable exit cone. These techniques cannot be used with tactical missiles. They are replaced by aerodynamic systems — fins — acting on the nozzle jet or, when the atmosphere is sufficiently dense, aerodynamic fins mounted on the case. Non-guided rockets require a spinning action to ensure flight stability. This requirement is taken into account when designing the nozzle. Various systems such as gas deflectors and slanted slots are included, which use the gas flow in the exit cone, or special motors are included to start the spin.
- Interface with the case, which must take into account the geometry selected — nozzle integration or maximum displacement of the nozzle — and the concern to minimize inert part mass.
- Performance, cost, reliability, environment and service life; often conflicting parameters which are used to select the final technical design.

In the case of ballistic and space missiles, performance requirements often lead to the design of materials with good thermal and mechanical stress characteristics, which are well suited for use in the production of large parts. There are currently three major families:

- Traditional composite materials (carbon-epoxy, glass-epoxy) for the body of the nozzle, sometimes replaced by metals (steel, aluminum).
- Ablative materials, made of refractory fiber reinforcements such as carbon, graphite and silica and a matrix obtained from the polymerization of a resin, generally phenolic. These materials are generally used for the duct and as insulation between the duct and the nozzle body.
- Thermostable insulators with a refractory matrix and ceramic or reinforcement carbon. They provide both insulation and structural integrity. They have no degassing at high temperatures and are used mainly for the nozzle walls. Carbon-carbon is particularly well suited for the manufacture of parts from a single block. It is composed of a carbon reinforcement (fabrics, fibers, pultruded sticks) and a carbon matrix obtained by a multistep liquid or gas process (densification process). It is known for its low density (1.5-2) and related excellent structural integrity at high temperatures. The design and development of new solid rocket motor (SRM) nozzles may incorporate these materials in several ways [15].

Frequently the entrance and throat region will be fabricated as a single piece of carbon-carbon material called an ITE (integral throat-entrance). A variation of this application is a single-piece throat, exit cone component called an ITEC or integral throat-exit-cone [16]. Carbon-carbon materials are used to construct very thin-walled structures for fixed and extendable segments of exit cones.

Finally a new concept is under development: the nozzleless solid rocket motor. This approach may use a high-strength, low-burn-rate propellant to form a nozzle. In this case [14], SRM cost reductions of 10-20% are expected.

1.2.5. *The ignition system*

The ignition system brings the energy necessary to the surface of the propellant to start burning. There are three stages:

- *Initiator*: a pyrotechnic element designed to transform an ignition signal such as shock, electrical impulse or light into the steady burning of a pyrotechnic substance.
- *Booster charge*: a charge, powder, pellets or propellant micro-rocket that transmits the flame between the primer and the main grain.
- *Main charge*: a charge, powder, pellets or propellant rocket that ignites the propellant grain.

Ignition systems for large propellant grains (ballistic missiles, space) use this three-stage process. The main charge burns for a few tenths of a second, delivering a discharge approximately a tenth of the flow rate of the propellant grain.

Ignition systems for small propellant grains are usually limited to a primer linked to a primary powder charge (instantaneous and very high release of gases during a few milliseconds) or a primer and an increment (a few tens of milliseconds).

The ignition materials have a high specific energy. They are designed to release either gases or solid particles, based on applications. Pyrotechnic ignition compounds include one or several generally metallic reducers, e.g., Al, Mg, B, Zn, C, and others, and one or several oxidizers or metallic oxides, e.g., NH_4ClO_4, CuO, Fe_2O_3, BaO, BaO_2, and others. Binary ignition compounds are the most used. Sometimes such compounds are designed to fit very specific applications, as was the case of the IFOC system (Initiateur à Fonctionnement par Onde de Choc; in English: shock wave primer), used on the Ariane rocket [17]. This compound is ignited by a shock wave and must not under any circumstances detonate.

2. Fundamental Equations of Internal Ballistics

2.1. INTRODUCTION

The objective of internal ballistics of propellant rocket motor is to provide the motor design engineer with the means to predict or understand the burning characteristics.

The following paragraphs provide a closer view of rocket motor operation. For more detailed information on the equations below, the reader is referred to classic books or technical papers [18-20].

To begin with, there are two fundamental definitions [21]:

- *Burning pressure*: this is the static pressure measured at the head end of the internal gas flow; in other words, it is the pressure at the forward end of the combustion chamber. It is, by definition, an absolute pressure.
- *Burning rate*: this is the linear regression rate of the flame edge, measured at a specific time and a specific distance on the propellant burning surface. The steady-state burning rate of a propellant (excluding the ignition phase and thrust tail-off) is defined by the ratio of minimum web to be burned (minimum distance traveled by the flame edge from the start of combustion to the time the flame reaches the outside contour of the grain) versus steady-state burning time. The burning rate is a function of the combustion chamber pressure.

2.2. PROPELLANT GRAIN FLOW RATE

For preliminary calculations it may be assumed that propellants burn in parallel layers, and that the burning rate is only a function of the pressure. Under these conditions the flow rate resulting from the combustion at a given time is:

$$q = \rho \cdot S \cdot v \tag{1}$$

where ρ is the density of the propellant, S the burning surface and v the burning rate of the propellant at a given time.

2.3. NOZZLE FLOW RATE AND DISCHARGE COEFFICIENT

A nozzle, like any other opening, allows a flow rate which is proportional to the opening area — here, the area of the throat, A_t — and to the pressure upstream of the nozzle — here, chamber pressure, p.

The proportionality coefficient is called the propellant discharge coefficient, indicated by C_D.

Where q' is the gas flow rate passing through the nozzle,

$$q' = C_D \cdot p \cdot A_t \tag{2}$$

where p is combustion pressure at a given time.

Presuming that gases are ideal, it can be shown [19,20] that coefficient C_D is affected only by the nature and temperature of the gases flowing through the nozzle, or

$$C_D = \frac{\Gamma(\gamma)}{\sqrt{\gamma r T}}; \quad \Gamma(\gamma) = \gamma \cdot \left(\frac{2}{\gamma + 1}\right)^{\gamma + 1/2(\gamma - 1)} \tag{3}$$

where:

T is the combustion temperature (ranging from 2000 to 3000 K);

γ is the ratio of specific heats of combustion gases at constant pressure and constant volume ($\gamma = c_p/c_v$ with an approximate value of 1.2);

r is $R/\mathcal{M}$ where R is the universal gas constant (8.134 J/kg·K) and $\mathcal{M}$ is the molar weight in kg (approximately 29×10^{-3} kg for propellant gases).

REMARK: T and γ are not very susceptible to pressure variations, particularly in the case of propellant with a low level of aluminum. Therefore, in many cases, the independence of C_D from pressure is accepted.

The discharge coefficient is expressed in seconds/meter, i.e. the inverse of the flow rate: meters/second. A typical value of C_D is in the range of 6.5×10^{-4} s/m. The average experimental flow rate coefficient is calculated by using eqn (4), which is obtained from eqn (2) by calculating the integral of both sides of the equation as a function of the burning time of the propellant grain:

$$C_D = \frac{M_p}{\int p(t) A_t(t)\, dt} \tag{4}$$

where M_p is the mass of propellant ejected and $p(t)$, $A_t(t)$, the equations for evolution of chamber pressure and of the nozzle throat area during combustion.

2.4. ROCKET MOTOR OPERATING POINT; KLEMMUNG (BURNING AREA TO THROAT AREA RATIO)

2.4.1. Operating point

The rocket motor operation point corresponds to the equality of the gas flow rates:

- created from the combustion of the propellant grain;
- ejected by the nozzle.

Based on eqns (1) and (2), this relation is given by:

$$\rho \cdot S \cdot v = C_D \cdot p \cdot A_t \tag{5}$$

REMARK: For preliminary calculations this equation does not take into account the volume of gas filling the space resulting from the combustion of the propellant inside the combustion chamber.

Relation (5) can also be written:

$$v = \frac{C_D}{\rho} \cdot \frac{A_t}{S} \cdot p \tag{6}$$

According to the above equations, at any given time in the combustion chamber of a rocket motor (A_t and S having values specific to the rocket motor) containing a known propellant (which defines C_D and ρ), the burning rate is proportional to pressure p.

The burning rate of a propellant, in terms of an intrinsic property of the material, is easily obtained by using small motors which have a constant propellant burning area S, and so a constant operation pressure p. (Refer to Chapter 4, Section 4). Within a common range of pressure (from 3 to 30 MPa depending on the propellant), several successive values may be obtained by selecting different values of the A_t/S ratio.

A law defined by the following equation:

$$v = ap^n (n < 1) \tag{7}$$

is often found to be a good expression of the phenomena.

The rocket motor operating point (v_o, p_o) at a given time will be such that eqns (6) and (7) are simultaneously validated.

On a graph with coordinates v and p (Fig. 3), the rocket motor operating

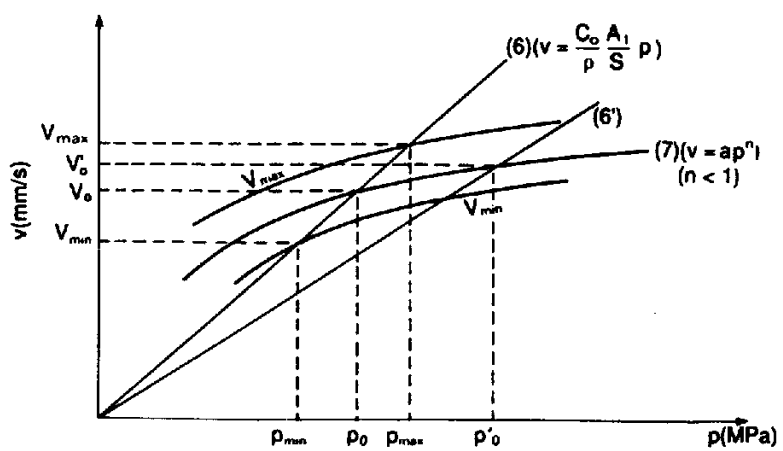

FIG. 1.3. Operating point of a rocket motor.

point is located at the intersection of the straight line of eqn (6) and the curve of eqn (7).

2.4.2. *Klemmung*

The klemmung of a rocket motor is the ratio between the propellant burning surface area and the throat nozzle area.

$$K = \frac{S}{A_t} \tag{8}$$

Equation (6) can be written in the form:

$$v = \frac{C_D}{\rho} \cdot \frac{1}{K} \cdot p \tag{9}$$

Figure 3 shows that for a given propellant grain (law $v = a\,p^n$ determined), the operating point of a rocket motor (v_o, p_o) is a function of the value of the klemmung.

Specifically, all other parameters being equal, a fluctuation in the value of K, either voluntarily induced to obey a thrust law or involuntary and deriving from an operational defect (e.g. a crack in the propellant grain causing a sudden increase of S, or a nozzle obstruction), results in a shift toward a new operating point corresponding to a new burning pressure (p'_o) and a new burning rate (v'_o).

2.5. USEFUL EQUATIONS

Equation (5) can be used in the form:

$$p = \frac{\rho \cdot S \cdot v}{C_D \cdot A_t} \tag{10}$$

effect of the burning law:

$$v = a \cdot p^n \, (n < 1)$$

Equation (10) can be used in the form:

$$p^{n-1} = \frac{\rho \cdot S \cdot a}{C_D \cdot A_t} \tag{11}$$

This last equation is useful for preliminary propellant grain design, excluding combustion phenomena covered in greater detail in Chapter 4.

With any given grain using a known propellant, there is:

ρ: constant;
a and n: presumed constant in the pressure zone analyzed;
C_D: presumed constant for the major part of the pressure rise of the combustion;
A_t: generally fluctuates so little that it can be assumed constant.

Relation (11) shows that, once the equation of the evolution of grain burning surface is known, the equation for propellant internal pressure can be determined, thereby demonstrating the importance of determining the initial burning surface, then calculating its evolution to be able to find the internal pressure law of the rocket motor best suited for the mission of the missile.

2.6. TEMPERATURE COEFFICIENTS

Propellant temperature affects the rate of burning. Because of the wide temperature ranges required for some tactical all-weather missiles, from −45°C to 60°C or more, a detailed knowledge of these variations is mandatory.

The equations for burning rate and pressure at various temperatures can be calculated from measurements. Curves v_{max} and v_{min} in Fig. 3 are an example of data obtained.

When characterizing the temperature sensitivity of a propellant, a constant klemmung ratio is generally preferred because it corresponds to a motor operating at various temperatures.

Coefficient π_K expressing the temperature sensitivity is written in the form:

$$\pi_K = \frac{1}{v} \cdot \left(\frac{\partial v}{\partial \theta}\right)_K$$

Approximately 0.25% for 1°C is a typical value found in composite propellants.

When v_{max} and v_{min} correspond to extreme temperature requirements for a tactical missile, Fig. 3 shows that the value of operating pressure can vary between p_{max} and p_{min} simply due to temperature changes.

Temperature sensitivity at constant pressure, π_p, is sometimes required. It is given by:

$$\pi_p = \frac{1}{v} \cdot \left(\frac{\partial v}{\partial \theta}\right)_p$$

with a burning rate law $v = ap^n$, it is easily demonstrated that:

$$\pi_p = (1 - n) \cdot \pi_K$$

3. Rocket Motor Thrust

3.1. THEORY OF OPERATION OF A NOZZLE

The nozzle expansion process involves the study of very complex transformations, chemical reactions, heat transfer, gas flow, etc.

Modelling the nozzle operation necessitates the use of simplifying assumptions that will lead to a model with results close to the actual performance of the rocket motor it represents.

Some aspects of this question have been covered in the specialized literature [18-20].

Some of the most important simplifying assumptions are:

- combustion and subsequent expansion of the combustion products are two separate phenomena that happen respectively in the combustion chamber and in the nozzle;
- the expansion in the nozzle is an isentropic phenomenon, in other words, adiabatic and reversible;
- one-dimensional flow;
- gas flow velocity at the entrance of the nozzle is very low and the gas kinetic energy is negligible;
- gas flow through the nozzle occurs without separating from the wall.

Combustion gases are known to remain in the nozzle for a period of 10^{-4} to 10^{-3} s; that information permits us to set the solution between two extreme models:

- the time needed to reach chemical balance is long compared with the time the gases remain in the nozzle; the gas composition does not evolve: it is a frozen equilibrium flow;
- the time needed to reach chemical balance is short compared with the time the gases remain in the nozzle; the gas remains in chemical equilibrium as a function of the local temperature and pressure through the expansion and in each area of the nozzle: it is a shifting equilibrium flow.

Working with the assumptions given above, a simplified method can be used by presuming that the combustion products are ideal with a constant molecular weight and γ.

Using the following variables:

p, T and ρ: pressure, temperature and density of the gases;
V: gas flow velocity;
A: a cross-section of the nozzle;
R: universal gas constant $\left(r = \frac{R}{\mathcal{M}}\right)$;

a: the speed of sound ($a = \sqrt{\gamma r T}$);
M: the Mach number ($M = V/a$);

and the following equations:

- the Mariotte law: $\frac{p}{\rho} = r \cdot T = \frac{R \cdot T}{\mathcal{M}}$
- continuity equation: $\rho \cdot A \cdot v = cst^e$
- Saint-Venant equation: $V^2 = 2 \cdot c_p \cdot \Delta T$
- Mayer formula: $c_p - c_v = r = \frac{R}{\mathcal{M}}$

and using the following subscripts:

- index 0: for the values of the parameters at the beginning of the convergent zone of the nozzle, in other words the values obtained during the propellant combustion;
- index t: for the values of the parameters at the throat of the nozzle;
- index s: for the values of the parameters at the exit plane of the nozzle;

The following is demonstrated:

3.1.1. The Hugoniot formula

$$\frac{dA}{A} = \frac{dV}{V}(M^2 - 1)$$

showing that, on a convergent-divergent nozzle:

- gas velocity increases continuously;
- gas velocity is equal to the speed of sound at the throat section ($M = 1$).

3.1.2. The existence of a maximum exhaust velocity

This velocity is reached through isentropic expansion of the gases, until absolute vacuum.

$$V_L = \sqrt{2 \cdot c_p \cdot T_o} = \sqrt{2 \cdot \frac{\gamma}{\gamma - 1} \cdot r \cdot T_o}$$

3.1.3. The existence of various relationships between the operational parameters

- In any section of the nozzle:

$$\frac{p}{p_o} = \left(\frac{T}{T_o}\right)^{\gamma/\gamma - 1} = \left(\frac{\rho}{\rho_o}\right)^{\gamma}$$

- At the nozzle throat:

$$\frac{p_t}{p_o} = \left(\frac{2}{\gamma + 1}\right)^{\gamma/(\gamma - 1)}$$

$$\frac{T_t}{T_o} = \frac{2}{\gamma + 1}$$

- At the exit cone section:

$$V_s = V_L \sqrt{1 - \left(\frac{p_s}{p_o}\right)^{(\gamma - 1)/\gamma}}$$

where p_o/p_s is the expansion ratio.

Because exhaust velocity is of primary importance in the determination of thrust, we need to write in its complete form:

$$V_s = \sqrt{\frac{2}{\gamma - 1} \cdot \frac{R}{\mathcal{M}} \cdot T_o \left[1 - \left(\frac{p_s}{p_o}\right)^{(\gamma - 1)/\gamma}\right]} \qquad (12)$$

where V_s increases when T_o does or when the molar mass $\mathcal{M}$ of the exhaust gases decreases.

3.2. DETERMINATION OF THE THRUST

Where p_a is the ambient pressure and q the gas mass flow rate of the nozzle:

$$F = q \cdot V_s + (p_s - p_a)A_s$$

This equation demonstrates:

- that thrust increases when ambient pressure (p_a) decreases. Thrust is maximum in vacuum, i.e.:

$$F \text{ vacuum} = q \cdot V_s + p_s \cdot A_s$$

- and that for a given ambient pressure (constant p_a) after taking into account the differential equation:

$$dF = V_s \cdot dq + q \cdot dV_s + A_s \cdot d(p_s - p_a) + (p_s - p_a) \cdot dA_s$$

where q and p_a are constant, thrust is maximum when $p_s = p_a$, that is:

$$F = q \cdot V_s$$

in which case we have the optimum expansion ratio of the nozzle; p_s is a function of p_o and of the geometry of the nozzle and, because of that, it cannot be constantly equal to p_a, which varies during flight.

- When $p_s > p_a$ the jet bursts at the exit cone. It is under-expanded.
- When $p_s < p_a$ the jet separates from the wall of the nozzle. It is over-expanded. (The Summerfield criterion, which is valid for the half-

angles of the exit cone of a nozzle smaller than 15°, indicates that separation occurs in an area where pressure is close to 0.4 p_a.)

3.3. THRUST COEFFICIENT

For practical reasons related to the design of the propellant grain, it is useful to use a proportionality coefficient, which is the ratio between the thrust on the one hand and the chamber pressure and throat area on the other hand. The relation is:

$$F = C_F \cdot p_o \cdot A_t \tag{13}$$

Combining with eqns (12) and (13), it is solved by:

$$C_F = \sqrt{\frac{2\gamma^2}{\gamma - 1} \cdot \left(\frac{2}{\gamma + 1}\right)^{(\gamma+1)/\gamma} \cdot \left[1 - \left(\frac{p_s}{p_o}\right)^{(\gamma-1)/\gamma}\right]} + \frac{p_s - p_a}{p_o} \cdot \frac{A_s}{A_t}$$

C_F is a parameter that does not depend on units of measure and depends solely on combustion gases (γ) of the ratio between sections $\varepsilon = A_s/A_t$ and on the ratio p_o/p_a. (p_o/p_s is expressed only as a function of γ and of A_s/A_t).

C_F indicates the efficiency of a nozzle for a given propellant grain and given nozzle geometry. Figure 4 shows the evolution of C_F as a function of the ratio $\varepsilon = A_s/A_t$ for various values for the p_o/p_a ratio.

These same results can be displayed in the form of tables, based on the values on γ.

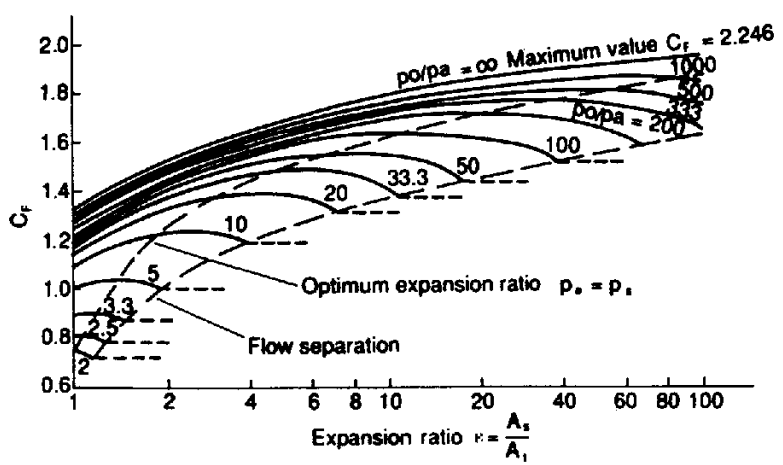

Thrust coefficient versus the expansion ratio for $\gamma = 1.20$

FIG. 1.4. C_F diagram.

4. Specific Impulse

4.1. INTRODUCTION

Suppose we have several rocket motors with identical structures (shape and equipment) and nozzles, and loaded with different propellant grains.

A comparison of their performance is easily done by measuring the intensity of the thrust F obtained by each of the motors during operation.

All things being equal, the various compositions of propellant grains can be compared by dividing thrust F obtained by the weight flow rate of propellant burned.

This ratio — the thrust obtained versus the weight flow rate — for a given rocket motor allows us to determine the intrinsic characteristics of the propellant grain used.

This is known as the specific impulse of the propellant grain. Because its dimensional equation is time, this value is expressed in seconds. At this point it is already clear that, because specific impulse can only be measured through the operation of a rocket motor, its experimental measurement is highly dependent on the rocket motor and its operating point.

4.2. DEFINITIONS AND RELATIONS

Instantaneous specific impulse is the ratio of thrust versus the weight flow rate of the propellant at a particular instant; it is given by:

$$I_s = \frac{F}{g_0 \cdot q} \tag{14}$$

where g_0 is the standard acceleration due to gravity ($g_0 = 9.80665$ m/s^2) and q the mass flow rate of the propellant.

From the previous equation we can write:

$$I_s = \frac{F}{g_0\, q} = \frac{p\, C_F\, A_t}{g_0\, p C_D\, A_t}; \quad I_s = \frac{C_F}{g_0\, C_D} \tag{15}$$

To measure performance of the propellant it is preferable, for practical reasons, to take into account total duration of combustion. By combining the second side of eqn (14) with the total combustion time (t_c), we obtain the average specific impulse of the propellant or of the rocket motor:

$$I_{sm} = \frac{\int_0^{t_c} F \cdot dt}{g_0 \int_0^{t_c} q \cdot dt} = \frac{\int_0^{t_c} F \cdot dt}{g_0 \cdot M_p}$$

where M_p is the total mass of propellant burned.

The integral of thrust F as a function of total combustion time (t_c) is called the total impulse of the rocket motor; it is given by:

$$I_{Ft} = \int_0^{t_c} F \, dt$$

Based on the preceding equations, we can deduce that:

$$I_{sm} = \frac{I_{Ft}}{g_0 \cdot M_p} \tag{16}$$

and

$$I_{Ft} = g_0 \cdot M_p \cdot I_{sm} \tag{17}$$

4.3. PRACTICAL APPLICATIONS

The definitions introduced in the preceding paragraph and related equations are used by the designers to guide them in the selection of the best performances.

4.3.1. *Propellant formulation*

Equation (15) shows a direct connection between specific impulse and nozzle discharge coefficient C_D. Based on the expression for C_D (see Section 2.3 of this chapter), we obtain a proportionality relationship between I_s and $\sqrt{T/\mathcal{M}}$. To design highly energetic propellants the researcher will seek the propellants with high combustion temperatures T that produce combustion gases with the lowest possible molar mass.

4.3.2. *Preliminary propellant grain design*

Preliminary design analyses of a rocket motor always require the determination of a thrust level F which must be available for a length of time t necessary to perform the assigned mission.

This requirement is translated into the level of total impulse to be obtained:

$$I_{FT} = F \times t.$$

Using eqn (17) and based on the value selected for the average specific impulse (I_{sm}), the expert is able to deduce the required weight of the corresponding propellant. This equation is of great use for all calculations for preliminary propellant grain design.

4.3.3. *Preliminary missile design*

A rocket with a total mass M moves vertically at a speed V. Where R is the resultant from aerodynamic forces expressing air drag and F the thrust delivered by the rocket motor, the equation of motion is:

$$M \cdot \frac{dV}{dt} = F + M \cdot g + R$$

$$M \cdot \frac{dV}{dt} = q \cdot g_0 \cdot I_s + M \cdot g + R$$

$$\frac{dV}{dt} = \frac{1}{M} \cdot \frac{dM}{dt} \cdot g_0 \cdot I_s + g + \frac{R}{M}$$

By integrating this equation between t_0 and t_1 which correspond to ignition and propellant burn-out ($t_c = t_1 - t_0$) and neglecting air drag the velocity increase is:

$$\Delta V = g_0 \cdot I_s \cdot \ln \frac{M_0}{M_1} + g \cdot t_c$$

Assuming that I_s and g remain constant during the t_c combustion time and where:

M_0 = total weight of the rocket ($M_0 = M_p + M_1$)
M_p = propellant weight
M_1 = rocket weight at burn-out

and

ρ = the density of the propellant
v = the volume of the propellant grain

we can write the following equation:

$$\Delta V = g_0 \cdot I_s \cdot \ln\left(1 + \frac{\rho v}{M_1}\right) + g \cdot t_c$$

All other things being equal (g, t_c), the velocity increase of the rocket is therefore a function of:

$$g_0 \cdot I_s \cdot \ln\left(1 + \frac{\rho v}{M_1}\right)$$

This equation is very useful for preliminary design analyses.

- When $M_p = \rho v$ is small compared to M_1 (the first stages of ballistic missiles), ΔV becomes a function of:

$$g_0 \cdot I_s \cdot \frac{\rho \cdot v}{M_1} \tag{22}$$

and the product $\rho \cdot v \cdot I_s$ is an important criterion for the comparison of propellant grains.

- When $M_p = \rho \cdot v$ is high compared to M_1 (the last stages of ballistic missiles), ΔV is a function of:

$$g_0 \cdot I_s \cdot \ln \frac{\rho \cdot v}{M_1}$$

in which case ρ intervenes only through its logarithm. Specific impulse alone is then an interesting criterion for the comparison of propellants.

These results suggest that propellants could be compared using a performance index such as:

$$I_s \cdot \rho^{\alpha} \quad \text{where } 0 < \alpha < 1$$

where α is dependent on the rocket motor in which the propellant is to be used. This theory has been developed in various references [18,22].

4.4. DETERMINATION OF THE AVERAGE STANDARD SPECIFIC IMPULSE

Experimental measurement of specific impulse is available only through operating a rocket motor. Consequently, its value is related to the rocket motor.

In addition, eqn (15):

$$I_s = \frac{C_F}{g_0 \cdot C_D}$$

shows that for a given propellant (γ constant), the value of I_s is dependent on C_F, therefore on the ratio of sections $\varepsilon = A_s/A_t$ and p_o/p_a which are inherent to the operating characteristics in the rocket motor.

These remarks illustrate why there is a certain amount of confusion concerning the comparison of the performance of propellants. To be fully convinced, it should be enough to note:

- that p_o is the internal operating pressure of the rocket motor and is therefore related to the combustion chamber characteristics;
- that p_a is the pressure outside of the missile and is therefore related to ambient test conditions;
- that ε is related to the geometry characteristics of the nozzle and their evolution during operation.

Luckily, it is commonly agreed that specific impulse is the parameter that should be used to discuss the performance of propellant grains or rocket motors. This means that, in practice, the exact operating conditions of a rocket motor must be established to allow measurement of the average standard specific impulse:

- The expansion ratio p_o to p_s has been established. Its value, in the United States, has been set at 68, where p_o is 1000 psi and $p_s = p_a$ is 14.7 psi (atmospheric pressure under normal conditions). In France, p_o was in the past assigned 70 atmospheres and a value of $p_s = p_a$ of 1 atmosphere; this ratio is therefore 70.
- The nozzle must be adjusted for the ambient pressure at sea level: $p_s = p_a = 0.10133$ MPa.
- The exit area is shaped like a cone with a 15° half-angle.

To obtain comparable data between propellants, the tests must be performed with identical rocket motors, known as standard rocket motors. The propellant grain geometries used are well suited to obtain the desired precise data (e.g. a combustion pressure that is as constant as possible, geometric parameters that are simple to measure, etc.).

Two types of geometry are commonly used; they are described in greater detail in Chapter 3, Section 5.5. They are:

- the 10-branch star-shaped propellant grains, named 'Mimosa';
- the cylindrical shape, a propellant grain from the United States, named 'Bates'.

These rocket motors are manufactured and tested very carefully to ensure good reproducibility and high-quality results. There may, however, still be some small differences from the standard operating conditions defined above. After analyzing the results, the necessary compensations are calculated; a detailed discussion of these corrective measures is found in Chapter 3, Section 5.9; they are based on the proportionality laws between specific impulse and thrust coefficient (C_F). The results of these measurements and calculations allow us to obtain the average standard specific impulse of the propellant, expressed by I_{sm}^{s}.

In conclusion, we see that great caution is necessary when discussing specific impulse. Indeed, a rigorous performance comparison between various propellants requires:

- identical rocket motors (shape, mass, insulation, shape and material of the nozzle, etc.);
- operating points corresponding to standard conditions;
- identical unit systems;
- test conditions and equipment sufficient to secure a good level of precision.

4.5. AVERAGE SPECIFIC IMPULSE OF A ROCKET MOTOR

For a given propellant it is possible to assess the performance of the future rocket motor by determining a predicted average specific impulse.

There are various methods to calculate and optimize the performance of a

rocket motor. An excellent synthesis of the research done by Working Group 17 under the AGARD (Advisory Group for Aerospace Research and Development) is available [23], in which the three main steps of this process are well described:

4.5.1. Calculation of the theoretical specific impulse of the propellant

This step uses the thermodynamics computer programs based on main algorithms developed by the Lewis Research Center of NASA [24]. In addition, there are two complementary data banks on thermodynamic properties of the various components of the propellants and other products likely to result from combustion and subroutines tailored to the needs of the user (presentation of results). The use of this software and various thermodynamic calculations performed are discussed in depth in Chapter 3.

Based on the chemical composition of the propellant, this software program calculates the various thermochemical characteristics of the combustion gases and the theoretical specific impulse of an ideal rocket motor having no losses, for the required operating point (p_o, p_a and ε). The major simplifying assumptions are:

- uniaxial, isentropic and non-viscous flow;
- chemical equilibrium of the gases during expansion;
- kinetic and thermal equilibrium between the solid and gaseous phases of the flow.

4.5.2. Determination of losses due to flow conditions in the nozzle

These losses result from the discrepancies between real properties of the flow of the gaseous mixture and the characteristics corresponding to the simplifying assumptions above. They belong, in general, to the following six categories:

- Losses through flow expansion because the flow is in fact bidimensional. They are a function of the half-angle of the exit cone and of its convex shape.
- Two-phase losses, resulting from velocity and temperature lag between the solid and the gaseous phases.
- Boundary layer losses, caused by the viscosity effect and by the heat exchange at the nozzle wall.
- Losses through chemical kinetics because of a delay in the establishment of chemical equilibrium of the gas flow.
- Losses due to the submergence of the nozzle into the propellant grain, resulting in a modification of the flow at the inlet of the nozzle.

- Losses due to erosion of the throat area through ablation, resulting in a decrease of nozzle expansion ratio.

4.5.3. Determination of losses due to chamber combustion conditions

With a radial burning propellant grain these losses are fairly limited compared to the losses due to the flow conditions in the nozzle. They are mainly caused by heat exchange at the walls and incomplete combustion.

The research done by Working Group 17 AGARD [23] permits comparison of the performance predictions done by various companies, using the steps described above. These forecasts were done for two different rocket motors. They were later compared to the experimental results.

Rocket motor	Average specific impulse forecast	Actual measurements
no. 1	289.6–294.5 s according to various companies	293.12 s
no. 2	292.8–299.1 s according to various companies	296.7 s

Complex programs are necessary to estimate the average specific impulse of a rocket motor. With such tools the designer is also able to improve the profile of the nozzle duct and, as a result, to optimize the performance of the rocket motor. The process involves successive iterations between profile modifications and calculation of corresponding losses, while at the same time taking into account the thermal characteristics of the materials.

4.6. EFFICIENCY

4.6.1. Propulsive efficiency

An estimation of the losses in the nozzle will be made experimentally by calculating the propulsive efficiency of the nozzle:

$$\eta_F = \frac{\overline{C_F}}{C_F}$$

with:

C_F obtained from the theoretical calculations described in the preceding section;

$\overline{C_F}$ obtained by using the firing data in the equation:

$$\overline{C_F} = \frac{\int F \cdot dt}{\overline{A_t} \cdot \int p \cdot dt}$$

where $\overline{A_t}$ is the average throat area during firing.

4.6.2. Combustion efficiency

Similarly, the combustion efficiency, which will indicate losses inside the combustion chamber, will be calculated by writing:

$$\eta^* = \frac{C_D}{\overline{C_D}}$$

with:

C_D obtained from the above theoretical calculation;
$\overline{C_D}$ obtained by using the firing data in the equation:

$$\overline{C_D} = \frac{M_p}{A_t \int p \cdot dt}$$

where M_p is the mass of propellant burned.

As a rule, losses inside the combustion chamber are limited and correspond to about 10% of the losses in the nozzle. This rule does not apply, however, to the end-burning propellant grains. In this particular case the importance of thermal losses in the combustion chamber increases with the regression of the flame front, leading to a drop of the specific impulse of the motor [25].

4.6.3. Overall efficiency of the rocket motor

The overall efficiency accounts for all losses in the rocket motor (nozzle and combustion chamber). It is written as a function of the average specific impulse:

$$\eta = \frac{I_{sm}\,(\text{measured})}{I_{sm}\,(\text{theoretical, without calculating the losses})}$$

Based on the equations described in this section, we see that:

$$\eta = \eta^* \cdot \eta_F$$

5. A Special Case: Ramjets and Ramrockets

5.1. GENERALITIES: AIR-BREATHING MOTORS

By definition, an air-breathing motor uses the oxygen in the air to function. Consequently, unlike rocket propulsion, a rocket engine using an air-breathing motor needs the outside environment to ensure its propulsion.

This type of motor is finding its application in the ramjet working technology which, in spite of a rather early design — proposed in 1911 by R. Lorin — is currently the object of renewed interest in the area of missile propulsion [26,27]. However, their operation assumes the use of boosters to allow reaching supersonic speeds.

During the propulsive phase of the ramjet the specific impulse (which is the impulse supplied by the mass unit of burned propellant), because of its use of atmospheric gases, is four to six times greater than the specific impulse of conventional propellants. These values are significant, however, only under operating conditions equivalent to those found during flight. For example, under specific experimental conditions (Mach 2, altitude 0) and a chamber pressure of 0.57 MPa, the average specific impulse will be in the range 1000–1300 s, depending on the propellant families.

5.2. DESCRIPTION OF A RAMJET

A typical ramjet includes the following components (see simplified drawing in Fig. 5):

- An air inlet, followed by a divergent diffuser section, located between sections 1 and 2, allowing the intake and compression (with temperature rise) of the quantity of air required for combustion.
- A fuel injection and air/fuel mixing system, located between sections 2 and 2′. For solid propellant motors, called ducted rockets or ramrockets, the liquid fuel is replaced by gases produced by the combustion of a propellant grain located in a primary chamber. The injection of these gases and their mixing with air takes place in an area located before the combustion chamber (Fig. 6).
- A combustion chamber where the mixture is burned, also called the secondary chamber (sections 2′ to 3), where the temperature rises (to approximately 2.200 K at 0.8 MPa in this particular case) at the same time as the gas flow increases.
- An ejection system for the combustion products through a convergent-divergent nozzle, assumed to be sonic at the throat (sections 3 to 5).

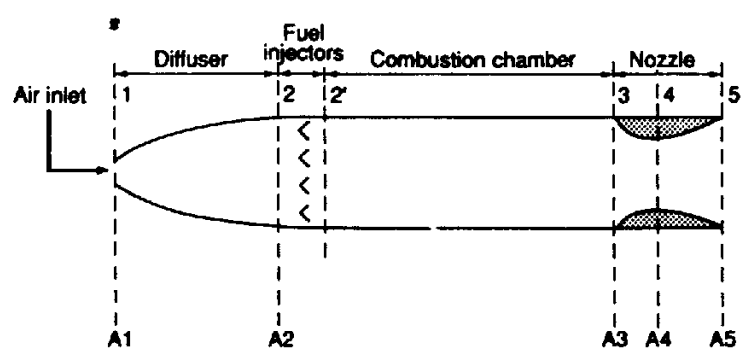

FIG. 1.5. Drawing of a ramjet.

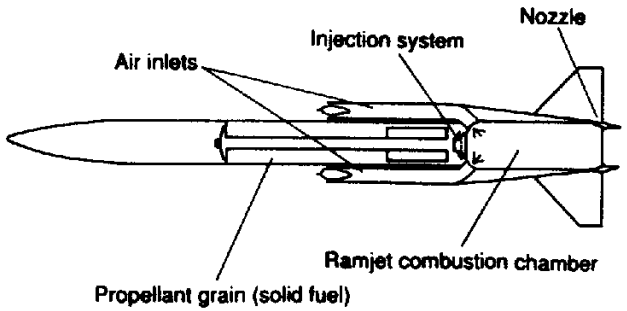

FIG. 1.6. Drawing of a solid-fuel ramjet.

To operate correctly, the ramjet must be ignited at supersonic speeds (around Mach 1.5). It has been clearly established that this method of propulsion is of no interest under Mach 1 beause the compression ratio is too low under such conditions.

5.3. PRINCIPLES OF OPERATION

Let us assume that the ramjet is a hollow axisymmetric shape, placed in a uniform supersonic flow with a velocity V_0 and equipped with an adjustable cover to allow variations in the exit plane A_4 (Figs 5 and 7).

Three types of operational modes are possible:

5.3.1. *Subcritical mode*

The cover is pulled back a little. The frontal shock wave is located in front of the inlet. A thin-stream jet of cross-section A_0 in front of the shock penetrates into the diffuser. When traversing the shock wave the flow becomes subsonic and is subjected to a recompression inside the diffuser. In the vicinity of the exit the flow accelerates and becomes sonic at S.

The resultant of the pressure force (internal pressure greater than external pressure) is directed toward the front, creating a thrust. The subcritical rate is characterized by a mass flow rate:

$$q_m = \rho_0 \cdot V_0 \cdot A_0 \tag{23}$$

5.3.2. *Critical mode*

The opening section S is further opened. The flow increases and the frontal shock wave moves closer to the inlet. The mass flow rate reaches its maximum value when the shock attaches itself to the rim of the air inlet:

$$q_m = \rho_0 \cdot V_0 \cdot A_1 \tag{24}$$

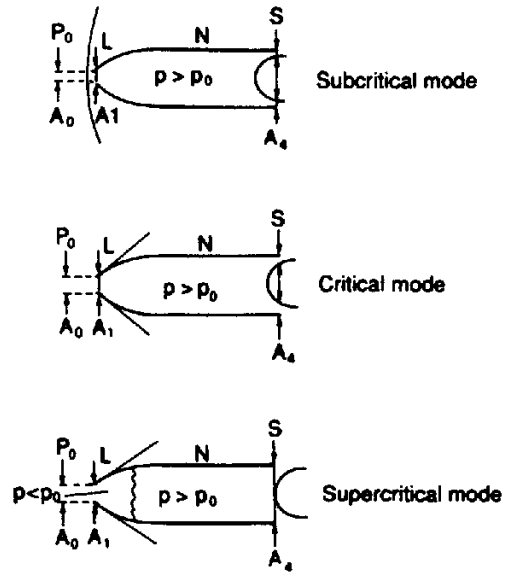

FIG. 1.7. Ramjet operating principles.

The flow in the diffuser is completely subsonic, the internal pressure remains greater than the external pressure. A thrust forward results. This operational rate corresponds to *optimal performance.*

5.3.3. *Supercritical mode*

When further increasing exit plane S, the external flow is not subject to any modification (constant rate q_m); the plane portion of the shock wave, however, moves into the diffuser. The thrust/drag balance is either positive or negative based on the position of the shock wave, because the internal pressure in front of and behind the shock is respectively smaller and greater than the atmospheric pressure.

5.4. EQUIVALENCE OF THERMAL AND MECHANICAL OBSTRUCTIONS

Removing the rear obstruction, and assuming that we supply a certain quantity Q of heat to the flow, between N and S: analyzing two neighboring sections of the flow between which dQ is supplied, a demonstration based on the classic laws of flow [28] leads to the equation:

$$(1 - M^2)\frac{dV}{V} = \frac{dQ}{T \cdot \rho}\cdot\frac{K^2}{a^2} - \frac{dA}{A} \tag{25}$$

where:

K^2 $= \dfrac{\partial p}{\partial s}$ (where s is the entropy of the flow gases);

a^2 = the square of the speed of sound;
V, ρ, p, T = velocity, density, pressure and temperature of the flow gases;
A = area of entrance section and M is the Mach number.

This equation shows that the addition of heat ($dQ > 0$) affects the velocity in the same way as a reduction of the cross-section ($dA < 0$), which explains the expression "thermal obstruction of the flow".

5.5. PROPULSION EQUATIONS

Looking at the ramjet in Fig. 5: conventional thrust is determined by applying the law of momentum [28,29].

$$F = p_5 A_5(1 + \gamma M_5^2) - p_o A_1 \varepsilon (1 + \gamma M_0^2) - p_o(A_5 - A_0) \qquad (26)$$

N.B.: The evolution of the value of a parameter is indicated with the value of its index, which stands for the section analyzed. The index i is used for generative pressure.

Assuming an operation at critical mode ($\varepsilon = A_0/A_1 = 1$) we use:

(1) Efficiency of the air intake

$$\eta_{o2} = \frac{p_{i2}}{p_{i0}}$$

(2) The characteristics of the motor rating

$$\eta_{25} = \frac{p_{i5}}{p_{i2}}$$

(3) The parameters of the geometry of the ejector

$$\sigma_{25} = \frac{A_5}{A_2} \text{ and } \frac{p_5}{p_{i5}} = \overline{\omega}(M_5)$$

where $\overline{\omega}(M) = \left(1 + \dfrac{\gamma - 1}{2} M^2\right)^{-\gamma/\gamma - 1}$

(for an isentropic expansion of a thermally ideal gas, γ is constant in permanent rating).

(4) The evolution of cross-section A of a stream tube

$$\frac{A}{A_c} = \frac{1}{M}\left(\frac{2}{\gamma + 1} + \frac{\gamma - 1}{\gamma + 1} M^2\right)^{\gamma + 1/2(\gamma - 1)} \equiv \sum(M)$$

where A_c (the critical area) indicates the surface that would be taken by this flow tube if the isentropic expansion reached $M = 1$.

(5) The equations

$$\frac{A_o}{A_{co}} = \sum_o \text{ and } \frac{A_2}{A_{c2}} = \sum_2$$

which, by writing the conservation of flow from infinitely upstream to section A_2 ($p_{io} A_{co} = p_{i2} A_{c2}$), leads to:

$$\eta_{o2} = \frac{p_{i2}}{p_{i0}} = \frac{A_1}{A_2} \cdot \frac{\sum_2}{\sum_o}$$

with the assumption ($\varepsilon = A_o/A_1 = 1$) which has been selected.

(6) External drag

$$X_{ext} = p_o(A_5 - A_o)$$

Equation (26) can be written:

$$\frac{F}{p_o A_2} = \eta_{o2}\left[\sigma_{25} \cdot \eta_{25} \cdot \frac{\overline{\omega}_5}{\overline{\omega}_o}(1 + \gamma M_5^2) - \frac{\sum_o}{\sum_2}(1 + \gamma M_o^2)\right] - \frac{X_{ext}}{p_o A_2} \qquad (27)$$

or:

$$\frac{F}{p_o A_2} = \eta_{o2} \cdot \mathcal{F} - \frac{X_{ext}}{p_o A_2} \qquad (28)$$

$\mathcal{F}$ depends solely on the geometry of the ejector (σ_{25}, M_5) on the flight Mach number and on the motor rating (η_{25}, M_2). Any increase $\Delta\eta_{o2}$ of efficiency in the air intake results, all other things being equal, in a proportional increase of the net thrust:

$$\Delta\left(\frac{F}{p_o A_2}\right) = \mathcal{F} \cdot \Delta\eta_{o2}$$

Finally, it is normal to use the value of thrust related to section A_5. A thrust coefficient is determined:

$$C_F = \frac{F}{1/2 \cdot \gamma \cdot M_o^2 \cdot p_o \cdot A_5}$$

In the case of critical operation, eqn (26) is used to write:

$$C_F = 2\left(\frac{p_5}{p_o} \cdot \frac{1 + \gamma M_5^2}{\gamma M_o^2} - \frac{A_o}{A_5} - \frac{1}{\gamma M_o^2}\right) \qquad (29)$$

Bibliography

1. BRUNER, G., La qualité métallurgique dans les industries aérospatiales, *L'Aéronautique et l'Astronautique*, 83, April 1980, pp. 13-18.
2. PARR, C. H., Composite for propulsion applications – an overview, 24th Joint Propulsion Conference, Boston, Massachusetts, AIAA-88-3127, July 1988.
3. DENOST, J. P., Conception des structures de propulseurs bobinées, *Design Methods in Solid Rocket Motors*, AGARD-LS-150, 1987, pp. 23-44.
4. LANGROCK, W. J., Solid rocket motor case design, *Design Methods in Solid Rocket Motors*, AGARD-LS-150, revised version 1988, pp. 1-16.
5. BADHAM, H. and THROP, G. P., Considerations for designers of cases for small solid propellant rocket motors, *Design Methods in Solid Rocket Motors*, AGARD-LS-150, 1987, pp. 1-20.
6. EVANS, P. R., Composite motor case design, *Design Methods in Solid Rocket Motors*, AGARD-LS-150, 1987, pp. 4.1-4.11.
7. GERLACH, H., Composite motor cases for tactical rockets, 24th Joint Propulsion Conference, Boston, Massachusetts, AIAA-88-3327, July 1988.
8. MAGNESS, R. W., Development of a high performance rocket motor for the VT-1 tactical missile, 24th Joint Propulsion Conference, Boston, Massachusetts, AIAA-88-3325, July 1988.
9. SOCIÉTÉ EUROPÉENNE DE PROPULSION, Brevet Français 83-15263, publication 2 552 494, 1983.
10. TRUCHOT, A., Conception et dimensionnement des protections thermiques internes d'un propulseur à poudre, *Design Methods in Solid Rocket Motors*, AGARD-LS-150, 1987, pp. 1-13.
11. YEZZI, C. A. and MOORE, B. B., Characterization of Kevlar/EPDM rubbers for use as rocket motor case insulators, 22nd Joint Propulsion Conference, Huntsville, Alabama, AIAA-86-1489, June 1986.
12. HILDRETH, J. H., Advances in solid rocket nozzle design and analysis technology in the United States since 1970, *Design Methods in Solid Rocket Motors*, AGARD-LS-150, 1987, pp. 1-15.
13. TRUCHOT, A., Conception et dimensionnement des tuyères de propulseurs à poudre, *Design Methods in Solid Rocket Motors*, AGARD-LS-150, 1987, pp. 1-27.
14. ALBERT, L., Nozzleless booster hardware demonstration progress to date, 24th Joint Propulsion Conference, Boston, Massachusetts, AAIA-88-3366, July 1988.
15. GENTIL, P., Design and development of a new SRM nozzle based on carbon-carbon and carbon-ceramic material, 24th Joint Propulsion Conference, Boston, Massachusetts, AIAA-88-3366, July 1988.
16. ELLIS, P. A., Testing of NOVOLTEX™ 3-D carbon-carbon integral throat and exit cones (ITECs), 24th Joint Propulsion Conference, Boston, Massachusetts, AIAA-88-3361, July 1988.
17. CHOTARD, P., Ignition by shock, Proceedings Fourth international pyrotechnics seminar, Steamboat Village, Colorado, 22-26 July 1974.
18. SUTTON, G. P., *Rocket Propulsion Elements*, 5th edn, Wiley, New York, 1986.
19. WILLIAMS, F. A., BARRERE, M. and HUANG, N. C., Fundamental aspects of solid propellant rockets, AGARDOGRAPH no. 116, Technivision Services, Slough, England, October 1969.
20. TIMNAT, Y. M., *Advanced Chemical Rocket Propulsion*, 1st edn, Academic Press, New York, 1987.
21. NAPOLY, C. and BOISSON, J., Paramètres d'autopropulsion, Laboratoire de Balistique, Sevran, no. 693, 1963.
22. Pire, Trajectoires phase propulsée, Trajectoires phase balistique, Engins balistiques et spatiaux à propergols solides, ADERA, St Médard en Jalles, 1985.
23. Report of the propulsion and energetics panel, Working Group 17, performance of rocket motors with metallized propellants, AGARD-AR-230, 1986.
24. GORDON, S. and MCBRIDE, B. J., Computer program for calculation of complex chemical equilibrium compositions, rocket performance, etc., NASA LEWIS, SP-273, 1971.
25. BANON, S. and ASTIER, J., The contribution of inert material to end burning propellant grain performances, 22nd Joint Propulsion Conference, Huntsville, Alabama, AIAA-86-1421, June 1986.

26. THOMAS, A. N. Jr, The outlook for ramjets and ramjet derivatives in U. S. military applications, AGARD Conference proceedings, no. 307, 1981, pp. 4.1-4.33. NATO Confidential.
27. MARGUET, R. and CAZIN, Ph., Ramjet research in France: realities and perspectives, 7th International Symposium on Air Breathing Engines, Beijing, People's Republic of China, ISABE-85-7022, September 1985, pp. 215-224.
28. CARRIÈRE, P., Aérodynamique interne des réacteurs, Ecole Nationale Supérieure de l'Aéronautique, Troisième année, Première partie: prises d'air, 1966, Troisième partie: statoréacteur, 1965.
29. CRISPIN, B., Ramjet and ramrocket. Propulsion systems for missiles. Introduction and overview, AGARD-LS-136, October 1984.